Transport in Porous Media

Spatial characterization of wetting in porous media using local lattice-Boltzmann simulations

--Manuscript Draft--

Manuscript Number:	TIPM-D-23-00185R1
Full Title:	Spatial characterization of wetting in porous media using local lattice-Boltzmann simulations
Article Type:	Original Research Paper
Keywords:	Wettability Contact angle Lattice Boltzmann method Digital rock modelling Multiphase fluid flow Porous medium
Corresponding Author:	Carl Fredrik Berg NTNU: Norges teknisk-naturvitenskapelige universitet NORWAY
Corresponding Author Secondary Information:	
Corresponding Author's Institution:	NTNU: Norges teknisk-naturvitenskapelige universitet
Corresponding Author's Secondary Institution:	
First Author:	Hamidreza Erfani, PhD
First Author Secondary Information:	
Order of Authors:	Hamidreza Erfani, PhD
	Reza Haghani
	James McClure, PhD
	Edo Boek
	Carl Fredrik Berg
Order of Authors Secondary Information:	
Funding Information:	Norges Forskningsråd (30141) — Dr Carl Fredrik Berg
Abstract:	Wettability is one of the critical parameters affecting multiphase flow in porous media. The wettability is determined by the affinity of fluids to the rock surface, which varies due to factors such as mineral heterogeneity, roughness, ageing, pore-space geometry, etc. It is well known that wettability varies spatially in natural rocks, it is still generally considered a constant parameter in pore-scale simulation studies. The accuracy of pore-scale simulation of multiphase flow in porous media is undermined by such inadequate wettability models. The advent of in-situ visualization techniques, e.g., X-ray imaging and microtomography, enables us to characterize the spatial distribution of wetting more accurately. There are several approaches for such characterization. Most include the construction of a meshed surface of the interface surfaces in a segmented X-ray image and are known to have significant errors arising from insufficient resolution and surface-smoothing algorithms. This work presents a novel approach for spatial determination of wetting properties using local lattice-Boltzmann simulations. The scheme is computationally efficient as the segmented X-ray image is divided into subdomains before conducting the lattice-Boltzmann simulations, enabling fast simulations. To test the proposed method, it was applied to two synthetic cases with known wettability and three datasets of imaged fluid distributions. The wettability map was obtained for all samples using local lattice-

	Boltzmann calculations on trapped ganglia and optimization on surface affinity parameters. The results were quantitatively compared with a previously developed geometrical contact angle determination method. The two synthetic cases were used to validate the results of the developed workflow, as well as to compare the wettability results with the geometrical analysis method. It is shown that the developed workflow accurately characterizes the wetting state in the synthetic porous media with an acceptable uncertainty, and is better to capture extreme wetting conditions. For the three datasets of imaged fluid distributions, our results show that the obtained contact angle distributions are consistent with the geometrical method. However, the obtained contact angle distributions tend to have a narrower span and are considered more realistic compared to the geometrical method. Finally, our results show the potential of the proposed scheme to efficiently obtain wettability maps of porous media using X-ray images of multiphase fluid distributions. The developed workflow can help for more accurate characterization of the wettability map in the porous media using limited experimental data, and hence more accurate digital rock analysis of multiphase flow in porous media.
Response to Reviewers:	The reply the reviewers is uploaded as a pdf file, with color coding. It is also glued in here: “Spatial characterization of wetting in porous media using local lattice-Boltzmann simulations” Hamidreza Erfani, Reza Haghani, James McClure, Edo Boek, Carl Fredrik Berg* November 5, 2023 Dear Prof Blunt, We appreciate the critical comments and suggestions mentioned by the respected reviewers and editor. All comments raised by the reviewers have been addressed in the manuscript or responded to. We hope that this new revision will further clarify these issues for the readers and make this manuscript a beneficial contribution to TiPM readers. In the end, we would like to thank you for your consideration and the constructive review process. Sincerely, Carl Fredrik Berg Reviewer #1: The manuscript presents novel approach for spatial characterisation of contact angle from pore-scale images of natural rocks with two fluid phases by performing isolated lattice-Boltzmann simulations for each particular ganglion. I find this manuscript interesting and believe that it has scientific contributions, however, I also believe that some important aspects should be clarified before recommending it for publication. The most important thing to me is that authors claim that proposed method is more ”accurate” (or more ”realistic”) than geometrical method previously published to which results are compare to. However, I do not find any strong scientifically valid proof that this is actually the case. Thus, I recommend a major revision where I believe that authors should provide more relevant validation with comparison between their method and geometrical analysis that was used in the manuscript. For example, using a single high-fidelity ganglia image, or creating artificial verification geometry, could be direction to take. However, I do believe that their statements regarding accuracy between two methods should be supported by some additional proof, or something that more clearly states pros and cons of each approach. Response: As suggested by the reviewer, we have now included a new section where

we have generated
an artificial image with known affinities. This new example does show that the proposed workflow yields
more accurate results for extreme wetting cases, as indicated by the previously considered experiments.
Additional comments are as follows:
1. There are multiple statements that proposed LBM method is computationally more efficient than
existing geometrical method, yet there are no any comparison of computational cost or further
discussion why this is the case.
Response: In the developed scheme the LBM model is running on individual ganglia independent
of other ganglia, thus the scheme is easy to parallelize. As we are running the LBM on a subdomain,
it is fast and not RAM-demanding. Since both methods are highly dependent on the implementa-
tion, we will not include numbers in the manuscript. For our given implementations the proposed
workflow is however significantly faster and requires much less memory.
2. Wettability map is obtained by LBM only for existing ganglia in the segmented images, while linear
interpolation is used to obtain contact angles for whole domain. What is physical relevance of doing
so? Understanding that obtaining wettability for whole domain is not trivial task to deal with and
that this is improvement considering that most studies still assume constant contact angle thought
domain, I still think that it would be valid point to discuss further and bring into context of realistic
heterogeneity of wettability.
Response: We appreciate the reviewer's comment. In this study we use direct numerical simula-
tions using LBM on isolated ganglia to obtain the wettability. Each simulation gives information
about the wettability of the considered three-phase contact line. So, aggregating all the informa-
tion for a snapshot (corresponding to a saturation) can give information for three-phase contact line
voxels of the sample. That we only obtain wettability along the three-phase lines holds irrespective
of the method, thus this is the case for both the geometrical method and our proposed method.
Even though, if the information of different μCT snapshots is assimilated we get more information,
still we miss the wettability of the majority of rock voxels. There are many options for how to
calculate the surface affinity for the voxels not located at the three-phase contact line, e.g., using
the closest neighbour or doing spatial 3D linear interpolation. The latter seems more realistic as it
uses more spatial information from neighbouring voxels.
3. In section 2, during LBM method description, explanations of some variables in equations are
missing. Moreover, I find order of writing an equation and calling them in text difficult to follow.
Response: We appreciate the comment. Section 2 has been rewritten, with definitions of missing
parameters added to this section. We hope that the reviewer finds the updated section more easy
to follow.
4. Line 211-212 states that having scalar affinity parameter is beneficial from optimisation standpoint.
Why is this? What would be beneficial comparing to other computational methods that

directly
use contact angle value?
Response: It is beneficial that the wettability is controlled by a single parameter. If wettability
was controlled by more parameters the optimization might not have a unique answer and more
iterations might be needed to converge to the global optimum answer for each ganglion. Optimizing
on affinity or the corresponding contact angle is of no consequence, as we simply relate them through
$\phi_s = \cos(\theta)$.
5. Even that is existing published method, section 2.3 should contain more details regarding geomet-
rical method as it is directly used for comparison with proposed LBM approach. Additionally,
more discussion regarding the uncertainty associated with geometrically measured contact angle is
needed as it is mentioned later without proper explanation.
Response: More explanation of geometrical contact angle measurement is provided in the revised
manuscript, while the original reference is also provided for deeper discussions. To avoid repetition,
we think the reader should be referred to the original reference for detailed formulation as the
algorithm is fully adopted from [1].
6. Line 245-247. I think that investigating a non-uniform wetting property of single ganglia could be
significant contribution to this work and potentially show additional benefit of proposed method.
Moreover, from this work, it is not clear if geometrical method uses uniform or non-uniform contact
angle for single ganglia.
Response: In this study, we only deal with assuming a single surface affinity for each ganglion to
show the proof of concept. Assuming spatial variation of wettability for a single ganglion is out
of the context of this study as it adds much more complexity, computational load and uncertainty
regarding the non-uniqueness of the optimization results.
To address this concern and show the improvement of the developed workflow over the geometrical
wettability characterization we added 2 numerical validation cases in Section 3. We think that this
provides a clearer view of improvement over the geometrical method as well as the accuracy of each
of the methods.
The geometrical method calculates a contact angle for each mesh-boundary along the three-phase
contact line (approximately on for each grid-cell along the three-phase contact line), thus it yields
different contact angles along the three-phase for a single ganglion. This has now been specified in
the text, see section 2.3.
7. Line 310 - add explanation of subscripts for oil and brine.
Response: This has now been added to the manuscript.
8. Section 2.5 - explain difference between unaltered and altered samples. Additionally, injection rates
in real units could be stated.
Response: This has now been added to the manuscript, see updated section 2.5.
9. Line 350 has typo: oil-wetting should be water-wetting.
Response: This is revised in the manuscript text.
10. Line 384 has typo: altered should be unaltered.
Response: We believe this should be ”altered”, the alteration renders the sample more oil-wetting.

11. Line 391-393. I don't see point of this statement. What is relevant here?
Response: This part compared the altered and unaltered contact angles obtained from both
schemes all together to compare them in the same plot. We expect the altered sample to show a
shift toward oil wetting behaviour compared to the unaltered sample. Surprisingly the unaltered
sample CA distribution from geometrical analysis is the same as the altered sample CA distribution
from the developed scheme.
12. Line 393-397 I would like see more discussion here as this is important point to make considering
the aim of the manuscript.
Response: We appreciate the reviewer's comment. Generally, we added more discussions to the
results and discussion section and also added section 33.1 with 2 cases for validating and comparing
the developed algorithm and geometrical analysis method results.

Reviewer #2:
1. It is recommended to start the abstract with general information about the topic.
Response: The abstract in the revised version opens with general sentences highlighting the
importance of the topic.
"Wettability is one of the critical parameters affecting multiphase flow in porous media. The
wettability is determined by the affinity of fluids to the rock surface, which varies due to factors
such as mineral heterogeneity, roughness, aging, pore-space geometry, etc. Despite that it is known
that wettability varies spatially in natural rocks, it is generally considered a constant parameter in
pore-scale simulation studies. The accuracy of pore-scale simulation of multiphase flow in porous
media is undermined by such inadequate wettability models."
2. It is suggested to discuss more about the findings of this study in the abstract.
Response: We added more findings to the abstract in the revised version. The changes in the
abstract can be followed in the annotated manuscript.
3. It is recommended to mention about the applications of this study at the end of abstract: The
findings of this study can help for better understanding of . . .
Response: We added this to the end of the abstract in the revised manuscript.
4. I strongly recommend the authors to add one paragraph discussing the difference between their
work and the previously performed studies in literature. In other words, what is the novelty of this
work? I offer the authors to revise the abstract and introduction in order to incorporate the novelty
of their work. This change motivates the readers of " Transport in Porous Media" to study this
work with interest.
Response: This is thoroughly discussed throughout the results and discussion section. We compare
our method extensively with the geometrical analysis method. We also added a new section to the
results and discussion (section 3.1) that we utilize two synthetic cases for validation and quantitative
comparison between the developed scheme and geometrical analysis.
5. It is recommended to include a paragraph at the end of introduction to present the steps of the
work like: First, the methods and materials are described. Then,. . .
Response: The last paragraph of the introduction serves this specific purpose in the revised

manuscript.
6. What are the advantages and disadvantages of this study? I recommend the authors to highlight
this topic. What are the limitations of this study? I recommend the authors to highlight this topic.
Response: We appreciate the reviewer's comment. We believe that this purpose is served through
the results and discussion section as well as section 2.4.
7. The quality of all the figures should be improved.
Response: All the figures are added to the manuscript as vector graphics to accommodate high-
quality and infinite zoom features.
8. It is recommended to add minor ticks (or intervals) on horizontal and vertical axis of all the plots.
Response: This is now added to all figures in the revised manuscript.
9. The title for last section should be changed to "Summary and Conclusions".
Response: This is now changed in the revised manuscript.
10. It is suggested to add a nomenclature (including alphabetic letters, Greek letters, subscripts, and
superscripts).
Response: We have done our best to define variables in their appropriate places. The nomenclature
will be mostly LBM parameters which is not the core contribution of the manuscript, we therefore
think that defining the parameters next to the equations will keep the main focus of the article
better.

Reviewer #3:
This paper proposes a workflow to characterize local wetting distributions in porous media using X-
ray images of two-phase fluid distributions. It first identifies isolated ganglia that are larger than a
specific size. These ganglia are then considered as initial guesses for lattice Boltzmann simulations.
The LB simulation is performed with different surface affinity values, and the single value that results
in a geometry with the minimum difference compared to the initial guess, determined through voxel-
by-voxel comparison, is considered the wettability of the contact line. This work is clear and to the
point, addressing an interesting problem and proposing an alternative workflow to determine wettability.
Although it is an interesting study, I still have a few concerns which I address below.
The image token was acquired under dynamic flow conditions, while the simulation was performed under
static conditions. This situation could lead to uncertainty in the determined surface affinity unless I am
misunderstanding something here.
Response: We appreciate the comment. We used 2 different experimental datasets to validate the
developed workflow. The first dataset is water injection into a core sample at residual gas saturation.
The other oil-brine experimental data are from steady-state co-injection of fluids into a sample with
1:1 volumetric ratio. In both conditions, we assume that the trapped ganglia are not moving, which
is realistic in a snapshot. As the surrounding fluid is moving around the ganglion, this can result in a
slight deformation compared to both fluids being stagnant. However, the capillary forces are assumed
strong compared to the viscous drag on the ganglion, we therefore do not expect large changes to a fully
stagnant case.

While assuming a single value for the surface affinity of each ganglion might be reasonable for small
ganglia, it could be inaccurate in cases where we have large ganglia that span a significant region.
Response: This is correct. It is a source of uncertainty and error in the current workflow, but for the
time being the most viable option was assuming a single value for each LBM simulation. If we wanted
to assume multiple local affinities for each ganglion the optimization calculations would be much more
expensive, and it might result in several local optima for the optimization. This is, however, a problem
that we will try to tackle in future work.
Could another method be employed to determine the spatial variation of wettability across the sample
instead of interpolation? Methods that can consider the spatial variogram?
Response: Any method can be employed in the stage of populating local wettability information to
the whole sample (all solid-fluid voxels). We chose simple 3D interpolation for the sake of simplicity in
this post-processing stage to avoid complications which might make the interpretation of results more
difficult.
Since all determined wettabilities are based on isolated ganglia, could this introduce bias in the simulation
compared to the geometrical method? I didn't understand if the geometrical results are solely based on
isolated ganglia or if any other three-phase lines are involved. Cause based on what was mentioned, the
percolating clusters or ganglia that cover a wide range of pore space and hold more interest cannot be
considered in this wettability analysis.
Response: This is absolutely correct. To avoid such bias the percolating ganglia were excluded from
the geometrical analysis as well and both methods were applied to the same ganglia. More explanation
is added to Section 2.4 for clarification.
Considering the method requires numerous lattice Boltzmann simulations, how does its computational
efficiency compare to other geometrical methods?
Response: The LBM simulations were run on a subdomain including a single ganglion so LBM simula-
tions are very RAM-efficient, but in the geometrical method, the whole solid-fluid and fluid-fluid surfaces
need to be meshed. Moreover, as the LBM simulations are independent of each other they can be easily
parallelized to be run at the same time. For our cases, the LBM method was faster. This is, naturally,
strongly dependent on the implementation, and might change with a more efficient implementation of
the geometrical method.
I might be mistaken, but in line 350, there appears to be a mistake. Do both distributions in Fig 4 display
oil-wetting behavior? Given that it's a gas-water system, should it exhibit water-wetting behavior instead?
Response: We highly appreciate the reviewer's comment. This was a typo in the manuscript and is
now revised. This sample was saturated with gas and water and the distributions show liquid wetting
conditions as expected.

References

[1] Hamid Hosseinzade Khanamiri, Per Arne Slotte, and Carl Fredrik Berg. Contact angles in two-phase

	flow images. Transport in Porous Media, 135(3):535–553, 2020.

Spatial characterization of wetting in porous media using local lattice-Boltzmann simulations

Hamidreza Erfani[a], Reza Haghani[a], James McClure[b], Edo Boek[c], Carl Fredrik Berg[a,*]

[a] *Department of Geoscience and Petroleum, Norwegian University of Science and Technology (NTNU), Trondheim, 7491, Norway*
[b] *Virginia Tech University, National Security Institute , Blacksburg, 24061, VA, USA*
[c] *Division of Chemical Engineering, School of Engineering and Materials Science, Queen Mary University of London Mile End Road, London, E1 4NS, United Kingdom*

Abstract

Wettability is one of the critical parameters affecting multiphase flow in porous media. The wettability is determined by the affinity of fluids to the rock surface, which varies due to factors such as mineral heterogeneity, roughness, ageing, pore-space geometry, etc. It is well known that wettability varies spatially in natural rocks, it is still generally considered a constant parameter in pore-scale simulation studies. The accuracy of pore-scale simulation of multiphase flow in porous media is undermined by such inadequate wettability models. The advent of in-situ visualization techniques, e.g., X-ray imaging and microtomography, enables us to characterize the spatial distribution of wetting more accurately. There are several approaches for such characterization. Most include the construction of a meshed surface of the interface surfaces in a segmented X-ray image and are known to have significant errors arising from insufficient resolution and surface-smoothing algorithms. This work presents a novel approach for spatial determination of wetting properties using local lattice-Boltzmann simulations. The scheme is computationally efficient as the segmented X-ray image is divided into subdomains before conducting the lattice-Boltzmann simulations, enabling fast simulations. To test the proposed method, it was applied to two synthetic cases with known wettability and three datasets of imaged fluid distributions. The wettability map was obtained for all samples using local lattice-Boltzmann calculations on trapped ganglia and optimization on surface affinity parameters. The results were quantitatively compared with a previously developed geometrical contact angle determination method. The two synthetic cases

*Corresponding author, carl.f.berg@ntnu.no

were used to validate the results of the developed workflow, as well as to compare the wettability results with the geometrical analysis method. It is shown that the developed workflow accurately characterizes the wetting state in the synthetic porous media with an acceptable uncertainty, and is better to capture extreme wetting conditions. For the three datasets of imaged fluid distributions, our results show that the obtained contact angle distributions are consistent with the geometrical method. However, the obtained contact angle distributions tend to have a narrower span and are considered more realistic compared to the geometrical method. Finally, our results show the potential of the proposed scheme to efficiently obtain wettability maps of porous media using X-ray images of multiphase fluid distributions. The developed workflow can help for more accurate characterization of the wettability map in the porous media using limited experimental data, and hence more accurate digital rock analysis of multiphase flow in porous media.

Keywords: Wettability, contact angle, lattice Boltzmann method, digital rock modelling, multiphase fluid flow, porous medium

---

1. Introduction

Multiphase simulation of flow and transport across different scales is relevant to a vast range of natural and industrial applications, e.g., enhanced oil recovery [1, 2, 3], geological CO_2 and hydrogen storage [4, 5, 6, 7], optimisation of fuel-cells operation [8, 9], industrial energy storage [10, 11], etc. The accuracy of continuum-scale multiphase modelling depends on constitutive relations such as relative permeability and capillary pressure. These can be obtained numerically using digital rock physics, or through time-consuming and expensive experimental procedures (i.e., core flooding, two-phase centrifuge, etc.) [12].

In recent decades, with improvements in X-ray tomography and other visualisation techniques, we can visualize inside porous media and characterise events, fluid distribution, and in-situ distribution of phases in porous media. Such advances helped us develop and verify digital rock physics techniques to simulate multiphase flow in porous media [12]. Hence, pore-scale models are a backbone of existing predictive models, either for phenomenological studies, upscaling of constitutive relations or avoiding experimental routines [13].

Recent developments in the realm of pore-scale modelling of multiphase flow focus on simulating flow through a realistic digital representation of complex pore space [14, 15]. It is well-understood that the pore structure in combination with fluid-fluid and solid-fluid interfacial forces governs the dynamics of multiphase flow and the geometry and morphology of phases [16, 17, 18]. The pore structure of porous media can be obtained with good accuracy using μ-CT X-ray imaging, additionally, there are well-established experimental methods to accurately measure fluid-fluid interfacial forces. In contrast, methods for assigning solid-fluid interfacial forces are not yet established. Fluid-fluid interfacial forces can often be considered constant throughout the simulation domain, and can therefore be described by simple models. Solid-fluid interfacial forces are usually imposed into the model using the wetting state of the solid wall and can have significant variation throughout the simulation domain, complicating its description [19].

Wettability is the relative preference of one fluid to coat the solid surface in the existence of another immiscible fluid, which is usually quantified by the contact angle [20]. The pore surface wettability determines the local balance of capillary forces and controls the local fluid distribution and morphology. The assignment of wettability to pore-scale models has long been recognised as having a strong impact on effective multiphase flow, and the lack of established methods has been recognised as the most significant issue for predictive multiphase modelling [21, 22]. This long-lasting challenge is still an area of debate, and the in-situ characterisation of wettability is still considered inaccurate [23].

Despite recent attempts, measuring in-situ contact angles on the fluid-solid-fluid (three-phase contact) line exhibits significant uncertainty and error due to contact angle hysteresis, effects of pore structure complexity, surface roughness, noise in image capturing, processing and segmentation [24, 25, 26]. The pore-scale observations of two-phase fluid flow can be averaged into an equilibrium contact angle for the whole sample [27], while it is well-known that the wetting state can be spatially variable in the pore space due to numerous reasons, e.g., mineralogy, clay coating, roughness, polar component coating, etc. [12, 28, 29, 30, 31].

Various approaches were followed by different researchers to measure local contact angles in porous media to make a wettability map instead of assigning a constant wetting property to the whole sample with the aim of a more accurate multiphase flow simulation. Most of the studies use geometrical approaches to measure the local contact angle on the three-phase contact line [32, 33, 34]. Deficit curvature of the fluid and solid interfaces have also gained significant attention recently [35, 36, 37]. Some studies used the extracted pore network of the sample to measure local wettability, e.g., Mascini et al. [38] used the extracted network of the sample to identify pore-filling events (Haines jump) to calculate local wettability [39, 40]. Garfi et al. [26] used the solid surface coverage in the pore regions to calculate the local wettability. Moreover, Foroughi et al. [41] used a pore-by-pore scheme to optimise the local wetting property using experimental dynamic X-ray tomography of capillary-dominated displacement in the porous media.

In this paper, we introduce a new automated workflow to characterise the local wetting distributions in porous media using X-ray images of two-phase fluid distribution. For the multiphase simulation, we use the lattice Boltzmann method (LBM), and the model of choice is called the colour-gradient model which was originally proposed by Gunstensen et al. [42] and modifications later on [43]. Yang and Boek [44] showed the capabilities of colour-gradient LBM to simulate the flow of binary fluids with high viscosity contrast and high numerical stability. In this model, the contact angle can be simply defined by an affinity parameter [43]. Simulations are conducted on isolated ganglia to get the wetting properties on the three-phase contact lines. Consequently, we have one LBM simulation for each ganglion, reducing the simulation domain and thereby improving the computational efficiency. We used a derivative-free optimisation scheme to minimize the difference between the fluid distribution from the LBM simulations and the imaged ganglia geometry by varying the surface affinity parameter in the colour-gradient LBM. Local wetting properties information was populated into the whole sample by a three-dimensional (3D) linear interpolation technique to construct a wettability map for the whole sample. Then, the proposed workflow was utilised to characterise the wettability of three publicly available datasets, and the obtained results were compared with geometrical curvature analysis.

This manuscript is organised as follows: In the next section, Section 2, we will present the methods used in this paper; the LBM method, wettability determination from geometrical analysis, and wettability determination through our introduced method using LBM simulations. We will also present three experimental data sets used for testing our introduced methodology. In Section 3, first we provide numerical validation, in which we compare the results of the developed workflow with the more traditional geometrical analysis method for contact angle calculation for two synthetic cases. Then, we will present the contact angle distribution obtained by applying the geometrical method and the introduced LBM simulation method for the three experimental cases. Further, we will compare and discuss the results. In the last section, Section 4, we summarize and conclude.

2. Methods and Materials

This section starts by introducing the methods used in this article and is followed by a presentation of the experimental data. The experimental data will be used in the next section to test our introduced methodology for wettability characterization. As our introduced methodology is based on LBM simulations, we start this section with a brief overview of the LBM method.

2.1. Colour-gradient lattice-Boltzmann model

The LBM is a computationally efficient and alternative approach to the classical computational fluid dynamics (CFD) methods to model flow and transport in complex geometries, which can be adapted to a wide range of applications. Models based on the LBM have been widely applied to study multiphase flow in porous media, with the colour-gradient model being the most popular implementation of two-fluid simulation [45, 46]. In this study, we used the LBPM open-source package [43], which is optimised to simulate incompressible immiscible two-fluid flows in μCT images of porous media. LBPM has routines to simulate unsteady displacement, steady-state flow at fixed saturation, and mimic centrifuge experiments [43]. Here we provide a brief introduction to lattice Boltzamnn (LB) formulation and wetting state implementation of the LBPM for the sake of completeness, and the readers are referred to McClure et al. [43] for more detailed formulation and in-depth discussion.

The colour-gradient LB model is defined based on three sets of lattice Boltzmann equations (LBE) to capture the interfaces between components a and b, and hydrodynamic properties. For incompressible immiscible mixture, the number density of two fluids, N_a and N_b, must be conserved. Two particle-distribution functions, A and B, are defined which are governed by the following LBEs:

$$A_q(\mathbf{x} + \boldsymbol{\zeta}_q \delta t, t + \delta t) = \omega_q N_a \left[1 + \frac{\mathbf{u}.\boldsymbol{\zeta}_q}{c_s^2} + \beta \frac{N_b}{N_a + N_b} \mathbf{n} \cdot \boldsymbol{\zeta}_q \right] \quad (1a)$$

$$B_q(\mathbf{x} + \boldsymbol{\zeta}_q \delta t, t + \delta t) = \omega_q N_b \left[1 + \frac{\mathbf{u}.\boldsymbol{\zeta}_q}{c_s^2} - \beta \frac{N_a}{N_a + N_b} \mathbf{n} \cdot \boldsymbol{\zeta}_q \right] \quad (1b)$$

where $\mathbf{x}$ and t are the space and time, respectively, δt is the time step and $\boldsymbol{u}$ is the flow velocity computed from hydrodynamic equations. The β parameter controls the thickness of the interface of the two components, and $\boldsymbol{n}$ is the unit normal vector of the interface. In the above equations, $\boldsymbol{\zeta}_q$ and ω_q are the microscopic velocity and the weighting factor in the q-direction of a lattice model, respectively. For our three-dimensional (3D) modelling, a seven-lattice velocity model (Q=7) is chosen for the above-mentioned equations, i.e., D3Q7. As such, the weights are $\omega_0 = \frac{1}{3}$, $\omega_{1,\ldots,6} = \frac{1}{9}$ and the microscopic velocities are the first seven directions in Eq. (6), i.e., $q = 0, \ldots, 6$. The speed of sound for this lattice is given by $c_s = \frac{\sqrt{2}}{3}$. The number density of the two fluids is computed by the zeroth-moments of the corresponding particle distribution functions:

$$N_a = \sum_{q=0}^{Q-1} A_q \tag{2a}$$

$$N_b = \sum_{q=0}^{Q-1} B_q \tag{2b}$$

A phase indicator field, ϕ, is defined to locate the interface by the density of the two fluids:

$$\phi = \frac{N_a - N_b}{N_a + N_b} \tag{3}$$

The unit normal vector of the colour gradient is calculated as

$$\mathbf{n} = \frac{\boldsymbol{\nabla}\phi}{|\boldsymbol{\nabla}\phi|} \tag{4}$$

In addition to the mass transport equation, momentum needs to be transported by an LBE to solve for two-fluid flow in porous media. A new particle distribution function, f, is defined which is governed by the following LBE equipped with the multi-relaxation-time (MRT) collision operator:

$$f_q(\mathbf{x} + \boldsymbol{\zeta}_q \delta t, t + \delta t) - f_q(\mathbf{x}, t) = \sum_{k=0}^{Q-1} M^{-1}_{q,k} S_k M_{q,k} (f^{eq}_k - f_k) \tag{5}$$

where M and M^{-1} are the orthogonal transformation matrix and its inverse, respectively [47], and S is the diagonal relaxation matrix containing the relaxation rates for each moment. Among the relaxation rates, the relaxation rate τ is related to the kinematic viscosity of the fluid with $\nu = c_s^2(\tau - 0.5)$, while the rest of the relation times are determined based on accuracy and numerical stability. Generally, the MRT collision operator is employed to perform the collision in a moment space instead of a discrete velocity space which results in higher stability in lower kinematic viscosities. The equilibrium distribution function, f_k^{eq}, and matrices M, M^{-1}, and S are defined in detail in McClure et al. [43], and their definitions are not mentioned here for the sake of briefness.

The hydrodynamic LBE (Eq. (5)) is solved on a popular D3Q19 lattice which is used by the LBPM package. For this lattice, the velocity set is

$$\boldsymbol{\zeta}_q = \begin{cases} \{0,0,0\}^T & \text{for } q = 0 \\ \{\pm 1,0,0\}^T & \text{for } q = 1,2 \\ \{0,\pm 1,0\}^T & \text{for } q = 3,4 \\ \{0,0,\pm 1\}^T & \text{for } q = 5,6 \\ \{\pm 1,\pm 1,0\}^T & \text{for } q = 7,8,9,10 \\ \{\pm 1,0,\pm 1\}^T & \text{for } q = 11,12,13,14 \\ \{0,\pm 1,\pm 1\}^T & \text{for } q = 15,16,17,18 \end{cases} \tag{6}$$

and the weights are $\omega_0 = \frac{1}{3}$, $\omega_{1,\ldots,6} = \frac{1}{18}$, and $\omega_{7,\ldots,18} = \frac{1}{36}$. The speed of sound for D3Q19 lattice is $c_s = \frac{1}{\sqrt{3}}$. By solving the LBE (Eq. (5)), one can determine the flow velocity based on the first moment of the distribution function:

$$\mathbf{u} = \frac{\sum_{q=0}^{Q-1} f_q \boldsymbol{\zeta}_q}{\sum_{q=0}^{Q-1} f_q} \tag{7}$$

This velocity is used in the mass transport equations, Eqs. (1).

2.2. Modelling wettability with lattice-Boltzmann models

One of the essential pieces of the multiphase flow simulation puzzle in porous media is the role of wettability, which affects flow on all scales. Therefore, it is important to allow for various implementations of wetting conditions to enable the simulation of different scenarios to be studied. There are various approaches for imposing wetting behaviour into LBMs [45]. In these models, the wetting characteristic can be applied as an upscaled property instead of taking the impact of different role-playing parameters like roughness, surface charge, film existence, etc. Note that some researchers used LBMs to study these effects on the upscaled behaviour of contact lines [23].

In the colour-gradient LBM, the wetting condition can be defined in the form of a scalar affinity value.It is demonstrated that the affinity value is equivalent to a pseudo-phase indicator field, ϕ_s, ranging from -1 to 1. It should be noted that the subscript s stands for the solid phase. This simple method imposes the expected contact line behaviour for the stationary and moving contact lines [48]. On a flat surface with a well-defined contact line, the equilibrium contact angle (θ_{eq}) is related to ϕ_s by

$$\cos\theta_{eq} = \phi_s \tag{8}$$

Note that ϕ_s equals the thermodynamically based wettability index $\omega_i = (\sigma_{bs} - \sigma_{as})/\sigma_{ab}$ introduced in [49], where σ_{as} and σ_{bs} are the surface tension between the solid phase and fluid a and b, respectively, while σ_{ab} is the interfacial tension between fluid a and b.

Figure 1 shows the relation between the surface affinity parameter and contact angle for a ganglion. In this study, we stick to the commonly used terminology and refer to the local wetting state as $\phi_s = 1$ being a strongly water-wet state and $\phi_s = -1$ being a strongly oil-wet state.

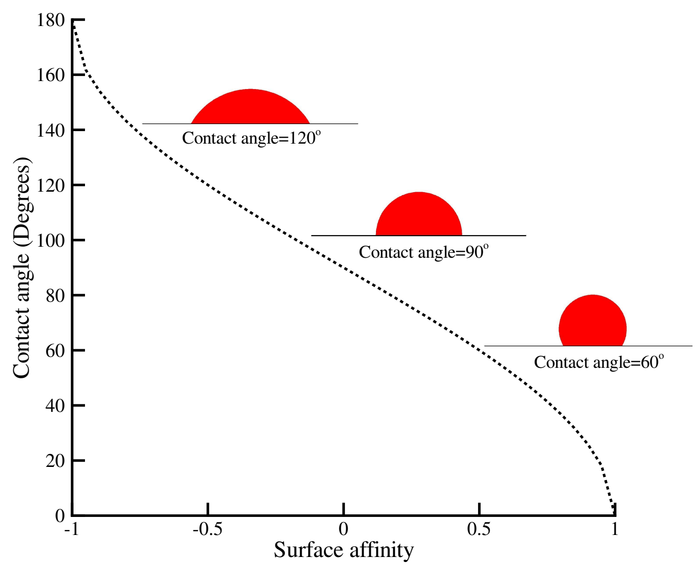

Figure 1: Contact angle (degrees) versus surface affinity parameter (ϕ_s) for a ganglion.

2.3. Geometrical contact angle determination

For geometrical contact angle measurements, we followed the automated method proposed by Khanamiri et al. [32] to calculate the contact angle along the three-phase contact line in the segmented experimental X-ray tomography data of two-phase fluid distributions. To calculate local curvature and contact angles, first, a triangulated mesh was applied to the fluid-fluid and solid-fluid interfaces of the segmented image. After correction for some artefacts in the generated mesh due to imaging resolution limitations, e.g., self-touching interfaces, the mesh was smoothed. The smoothing was applied following the method suggested by AlRatrout et al. [50] with some modification, in which the vertices are displaced to minimize the curvatures while keeping the global phase volumes approximately constant [51]. In the smoothing procedure, some tuning parameters are used which may result in the divergence of meshes from the intended geometry. As such, the final mesh may not imitate porous structures in low-resolution images, and as a result, the measured properties such as the measured contact angle and the curvature can deviate [32].

After smoothing the mesh, the contact angle between the solid-fluid and fluid-fluid meshes on a vertex on the three-phase contact line is calculated by the dot product of the unit normal vectors of the solid-fluid and fluid-fluid interfaces. Note that the geometrical contact angle method yields different contact angles along the three-phase contact line. As will be described in the next section, our proposed method yields a single affinity value for each ganglion.

Also, the local average curvature for an interface is calculated based on the dot product of the Laplace-Beltrami operator [51] and the unit normal vector. Further details of the geometrical method can be found in Khanamiri et al. [32]. They showed that to have a good estimation of the mean contact angle, the fluid clusters with at least a few thousand vertices at the fluid-fluid interfaces should be considered for the computation. By investigating two analytical examples with known contact angles and curvatures, they found that the computed point-wise contact angles, average mean curvature, and interfacial area converge by increasing the grid resolution (or increasing the size of clusters) while the point-wise mean curvature does not converge.

2.4. Wettability characterisation workflow

In this study, we propose a novel workflow to characterise the local wetting properties in a sample under two-phase conditions using local LBM simulation on individual ganglia. The procedure starts with a segmented image of a sample containing two immiscible phases. We assume that all interfaces are stagnant, either under steady-state conditions (i.e., the flow takes place

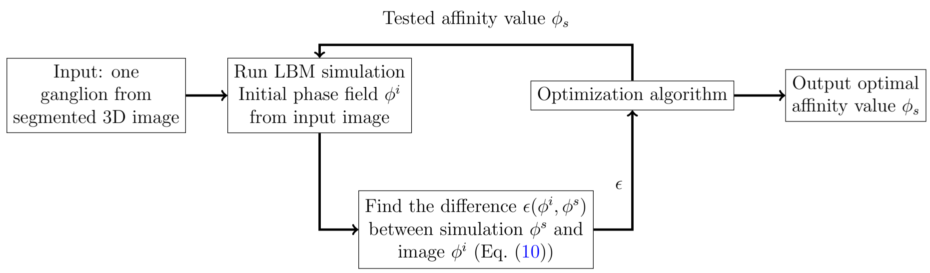

Figure 2: A flowchart of the optimization loop, finding the affinity value ϕ_s that minimizes the difference ϵ in the phase field between the imaged ganglion ϕ^i and the simulated one ϕ^s.

in connected pathways of phases from the inlet to the outlet), or the injection of fluids is stopped and the image is taken after equilibration of phases inside the sample. Moreover, we assume that the wetting property along the three-phase contact line is uniform, so that each ganglion is associated with a single tuning parameter (i.e., surface affinity) for a more robust optimisation procedure.

The first step in our workflow is the identification of all trapped ganglia of the phase with lower saturation in the sample and disconnected from the boundaries of the image. In the gas-water sample, we found the trapped ganglia of the gaseous phase, while in the oil-water samples, we found the trapped ganglia of the oil phase. In both cases, we then identified the trapped ganglia of the non-wetting phase. When we identify the ganglia of the non-wetting phase, we consider two voxels connected if they share a face. This ganglia labelling was conducted using the `scipy` Python-library, giving each ganglion a specific number. We only considered ganglia of size larger than 10 voxels, removing all ganglia smaller than this cut-off value from our set of ganglia. This cut-off value is arbitrary, however, including smaller ganglia than 10 voxels seemed to increase the noise in our results.

The optimization procedure for finding the wetting of a single ganglion is outlined in Fig. 2. In this optimization procedure we first find the smallest rectangular cuboid encapsulating the ganglion under consideration, and then enlarge this domain by five voxels in each direction to ensure that the ganglion is not interacting with the domain boundaries. Then we set all fluid voxels outside this ganglion to the wetting phase, so that the ganglion contains all non-wetting phases inside the domain. We then initialise the LBM from this fluid distribution, so that we have the initial phase field $\phi^i = 1$ for all wetting phase voxels and $\phi^i = -1$ for non-wetting phase voxels. In other words, the phase field is -1 inside the considered ganglion and 1 outside.

The optimisation parameter for each set of simulations (i.e., each ganglion) was the surface affinity parameter, ϕ_s, and the optimisation was performed with a derivative-free algorithm (Nelder-Mead). For a given surface affinity value ϕ_s provided by the optimization algorithm, we associate all solid surface faces with this affinity value. We then performed an LBM simulation inside the domain with no flow boundary conditions until we achieved a relaxed system. From the relaxed system, we binarised the phase field as:

$$\phi^s = \begin{cases} 1 & \text{if } \phi \geq 0 \\ -1 & \text{if } \phi < 0 \end{cases} \tag{9}$$

Note that the initial phase field is already -1 for voxels containing the non-wetting phase and 1 for voxels containing the wetting phase. We then calculated an error function from a voxel-by-voxel comparison of the simulated ganglion ϕ^s with the initial X-ray image geometry of the ganglion as given by ϕ^i:

$$\epsilon = \epsilon(\phi^i, \phi^s) = \sqrt{\frac{1}{|\Omega|} \int_\Omega (\phi^i - \phi^s)^2 dV} \tag{10}$$

where Ω is the pore space of the rectangular cuboid domain. After convergence of the optimisation loop, the obtained affinity value is assigned to the 3-phase contact line voxels in the X-ray image before moving to the next ganglion.

After optimising the surface affinity values for all ganglia, we obtained surface affinity values along all three-phase contact lines for these ganglia. These surface affinity values can then be translated to contact angles, using Eq. (8), for comparison with contact angle values obtained using the geometric method. Noteworthy, to make the comparison between the geometrical analysis and the developed workflow consistent, the percolating ganglia were excluded from the geometrical analysis as well. For this purpose, a new domain only including the analysed ganglia in the wettability characterization workflow was generated and fed into the geometrical analysis model.

For multi-phase flow simulations, a wettability map on all solid surfaces is required. While this is typically given as a single value, our workflow enables the distribution of wettability according to the obtained affinity values from the workflow outlined in Fig. 2. For this end, we populate all solid-fluid voxels of the segmented X-ray image using three-dimensional linear interpolation between the solid-fluid voxels on the three-phase contact lines, as these surfaces on the three-phase contact lines already have assigned surface affinity values from the workflow above. For the pore surface close to the boundaries of the domain, where the three-dimensional linear interpolation has insufficient data, the surface affinity value was chosen equal to the nearest point with an assigned value.

2.5. Experimental datasets

We used three publicly available experimental μ-CT datasets of imaged two-phase fluid distributions to assess the results of the developed wettability characterisation workflow. These datasets were also used by other researchers for similar purposes which gave a good benchmark to compare our obtained results.

Gas-water Bentheimer sample: This dataset was originally obtained by Sun et al. [35] and was used to get the wetting state using their theoretical development of geometrical analysis. A bench-top helical μ-CT scanner was used to image the 3D configuration of air-water immiscible fluids under ambient conditions in an untreated Bentheimer sandstone sample (4.9 mm in diameter and 10 mm long). The sample was flooded with brine with an injection rate of 3.3×10^{-7} m/s until irreducible air saturation was obtained ($S_w = 0.93$). The images were acquired with a resolution of 4.95 μm and we used a sub-volume of $720 \times 891 \times 891$ voxels from the segmented image.

Oil-water Bentheimer samples (unaltered and altered): These datasets were previously created from laboratory observations and discussed by Lin et al. [52, 53], and recently used by Garfi et al. [26] for the spatial distribution of wettability. These datasets consist of extensive sets of quasi-static co-injection at different fractional flows of oil (decalin) and water phases in cylindrical rock samples (diameter of 6.1 mm). The brine fraction of flow $f_b = Q_b/(Q_b + Q_o)$ was defined as the ratio of the brine injection flow rate, Q_b to the total injection rate, $Q_b + Q_o$, where Q is the injection flow rate and b and o subscripts denote brine and oil phases, respectively. For the unaltered sample, the oil phase (decalin) drainage was performed into the brine-saturated sample using centrifugation to reach irreducible water saturation. The imbibition was performed right after drainage in capillary dominant condition [54]. Brine imbibition was conducted in seven steps, increasing the fractional flow of brine from 0 to 1 (f_b=0, 0.05, 0.15, 0.30, 0.50, 0.85, 1). The injection was continued until reaching the steady state, and once the pressure difference across the sample was equilibrated the μ-CT images were acquired for each fractional flow with a resolution of 3.58 μm. For the altered sample, the fractional flows were performed for f_b=0, 0.02, 0.06, 0.24, 0.50, 0.80, 0.90, 1.

The aging process applied to the modified Bentheimer dataset occurred between the drainage stage and the co-injection fractional flow stages of oil and brine. Following the drainage phase, the sample was placed in crude oil, causing decalin to be gradually replaced by crude oil through diffusion. The sample was then kept in crude oil for 30 days at a temperature of 80 °C. Following this modification process, the sample was immersed in decalin to replace the crude oil. Afterwards, the coreflooding experiment was conducted. The composition of brine and more detail regarding the aging process for the altered sample can be found in Lin et al. [52, 53]. For both datasets, our analysis was performed on a cubic region of 800^3 voxels corresponding to 2.86^3 mm^3, of the image acquired for the fractional flow of f_b=0.5.

3. Results and Discussion

In this section, we provide the obtained results and discuss the differences with geometrical analysis of the oil ganglia to obtain the wetting properties of the natural rocks filled with two fluid phases. Firstly, we present a simplified example for numerical validation, then we provide the results of Bentheimer sandstone with gas-water fluids, and finally, we discuss the results of water-wet and altered-wet (mixed-wet) sandstone samples with oil-water pair of fluids.

3.1. Numerical validation

In this section, we provide numerical experiments for the validation of the developed workflow as well as compare the accuracy with the geometrical analysis contact angle measurement. For this purpose, two different cases were generated using two-phase colour LB simulations with surface affinities of $\phi_s = 0.5, 1$, where each case consisted of the same set of initial ganglia in a porous medium of 100^3 voxels as shown in Figure 3(a). The domain was then relaxed by LBM under no-flow conditions for the two surface affinities. To mimic the added noise and uncertainty of the imaging and segmentation process of experimental imaging of porous media, a median filter was applied to the simulated domains that introduce differences compared to the higher resolution LBM simulation results. Figure 3 depicts the initial domain with patches of the non-wetting phase, as well as the obtained numerical simulation results for $\phi_s = 0.5$ and $\phi_s = 1$. Finally, the wettability of the results was characterized by the developed workflow as well as the geometrical method to quantitatively evaluate the accuracy of each method based on initial input.

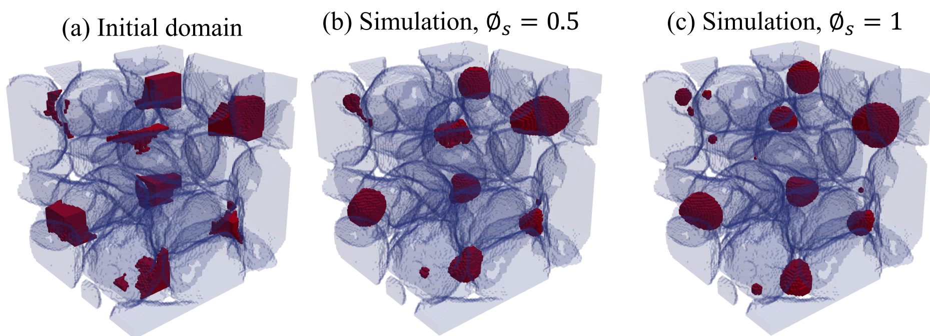

Figure 3: Numerical simulation of the two-phase static condition using the LBM. (a) Initial condition, a porous media of 100^3 voxel size, saturated with fluid 1 with patches of fluid 2 (non-wetting fluid, red colour). (b) final result for relaxation of the domain using $\phi_s = 0.5$, and (c) final results using $\phi_s = 1$.

Figure 4 shows the results of both the developed workflow and the geometrical analysis for these two cases. As it can be seen the geometrically obtained contact angles have a wider range. This is as expected due to the central limit theorem since the proposed method yields one single value for a ganglion, which corresponds to a value for each grid cell along the three-phase contact line for the geometrical method. The geometrical method yields a fair estimate for the $\phi_s = 0.5$ model but struggles to capture the affinity values for the $\phi_s = 1$ case. The results of the developed workflow are more representative of the high-affinity case of $\phi_s = 1$.

For the case with the surface affinity of 1 (i.e., $\phi_s = 1$, strongly non-wetting case) the geometrical analysis contact angles results range mostly from 0 to 60 degrees with an average of 37.5 degrees. For the case with $\phi_s = 0.5$ the obtained geometrical contact angles range from 37 to 90 degrees with an average of 60 degrees. On the other hand, the developed workflow gave a range of affinities for each case with averages of $\phi_s = 0.95$ and $\phi_s = 0.70$ for these two cases, corresponding to contact angles of 18 and 46 degrees, respectively. The presented results show that the wettability characterization results can be more representative using the developed workflow than the geometrical analysis method for the presented cases.

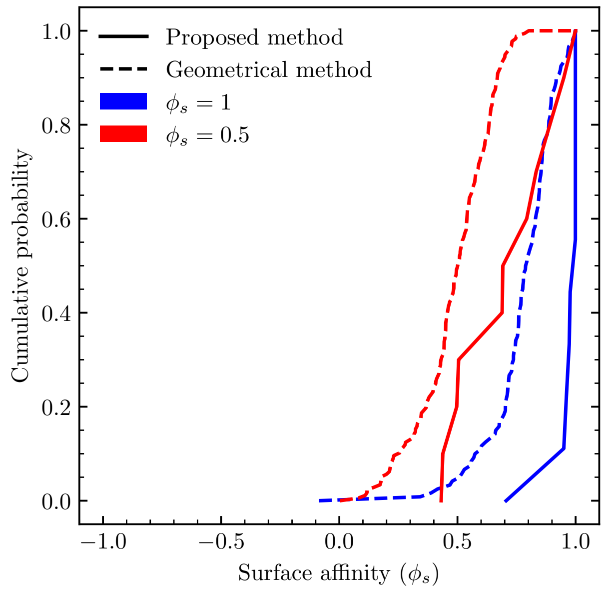

Figure 4: Obtained affinity value distributions for both the proposed method and the traditional geometrical analysis for the two simulated domains using lattice-Boltzmann simulations ($\phi_s = 0.5$ and $\phi_s = 1$, corresponding to contact angles of 60 and 0 degrees).

3.2. Gas-water Bentheimer sample

The first experimental dataset that we used to examine the proposed scheme for wettability characterization of two-phase fluid distribution was the Bentheimer sample saturated with water and gas fluid pair under no-flow boundary conditions in ambient pressure and temperature. The existence of water and gas together is beneficial as it is well-known that gas is usually the strongly non-wetting phase in such conditions. Figure 5(a) shows the obtained distribution of surface affinity parameter (ϕ_s) for this sample. For the proposed wettability characterization scheme in this research, each ganglion gives a data point as the local simulation was performed on each disconnected gas ganglion and the surface affinity parameter was optimized based on how well the lattice-Boltzmann model described the geometry of that specific ganglion. The obtained distribution is significantly shifted toward the liquid-wetting end of the spectrum with most of the ganglia being well described with ϕ_s=1 which is the strongly non-wetting condition for the gas phase.

The geometrical algorithm gives multiple calculations along the three-phase contact line, to examine such effect in the proposed scheme surface affinity distribution we also plot the distribution of surface affinity weighted by the ganglion size in Figure 5(b). As can be seen, compared to Figure 5(b) weighting the surface affinity by the size of the ganglion does not materially change the obtained distribution for the surface affinity. So, in the remaining part of the paper we stick to unweighted distributions for the proposed wettability characterization scheme to highlight the differences with geometrical analysis.

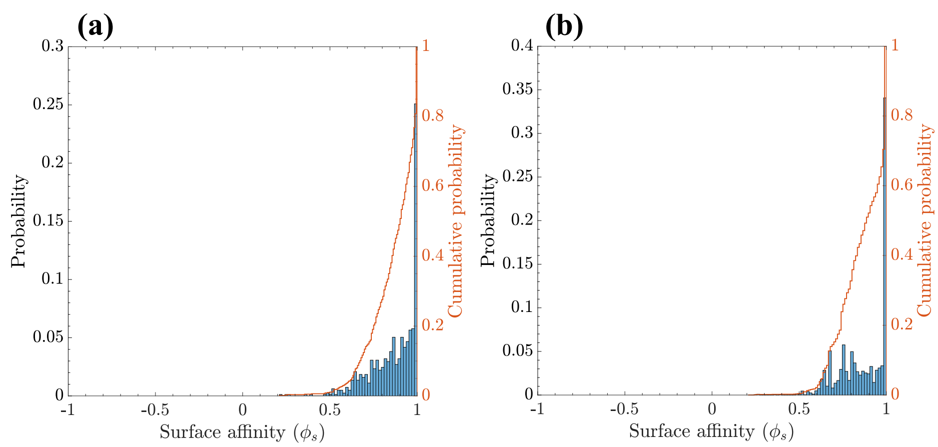

Figure 5: The distribution of surface affinity parameter (ϕ_s) for different ganglia in gas-water Bentheimer sample. (a) Unweighted distribution, (b) weighted distribution by the size of ganglia.

To be able to directly compare the proposed method for wettability characterization using LBM with the geometrical analysis we converted the obtained ϕ_s distribution to the contact angle, shown in Figure 6. Both distributions show the water-wetting behaviour of the sample as expected while the proposed scheme characterizes the wettability as strongly liquid wetting, with most of the contact angle distribution being in the range of 0-45 degrees. On the other hand, the geometrical analysis contact angle distribution provides a wider span with the peak of the distribution at around 60 degrees, which is unexpected for the water and gas in the porous media in ambient conditions. As the geometrical analysis is a local numerical approach that calculates the contact angle based on the orthogonal vector of solid-fluid and fluid-fluid surfaces it is more prone to local artefacts, roughness, and abnormalities in imaging or natural rock surface. Moreover, Figure 7 shows one of the observed ganglia in the porous media together with the simulated region for different affinities. In this specific case, the optimization algorithm converged to ϕ_s=0.724 which provides the best description of the cluster.

Figure 8 depicts the obtained wettability distribution map (i.e., ϕ_s) for all solid-fluid voxels in the gas-water Bentheimer sample. The voxels are not shown for the top half of the sample for the sake of better visualization of the spatial distribution of the trapped gas ganglia in the sample, which gives the wetting properties of the sample.

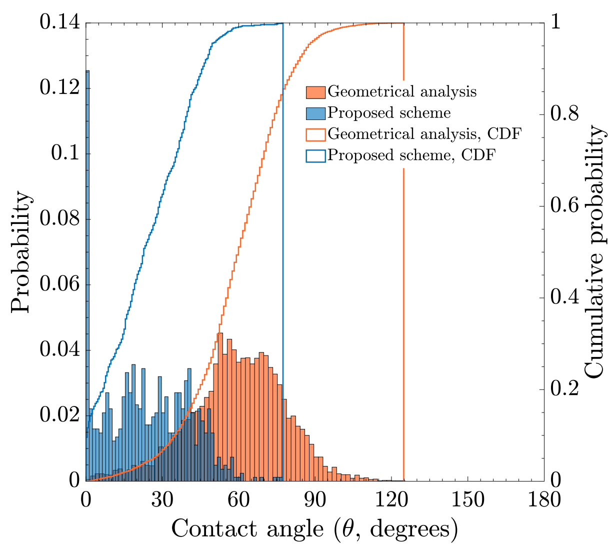

Figure 6: Obtained contact angle distributions for geometrical analysis and the proposed scheme for the gas-water Bentheimer sample.

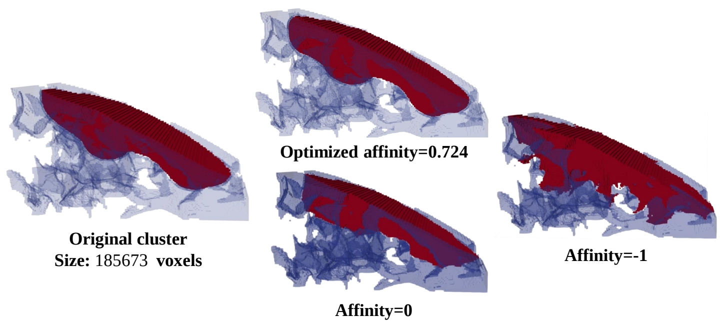

Figure 7: One of the trapped gas ganglions in the gas-water Bentheimer sample and simulation cases for different surface affinity values using local LB simulations. For this cluster, the final optimized value of surface affinity is ϕ_s=0.724 which describes the cluster the best.

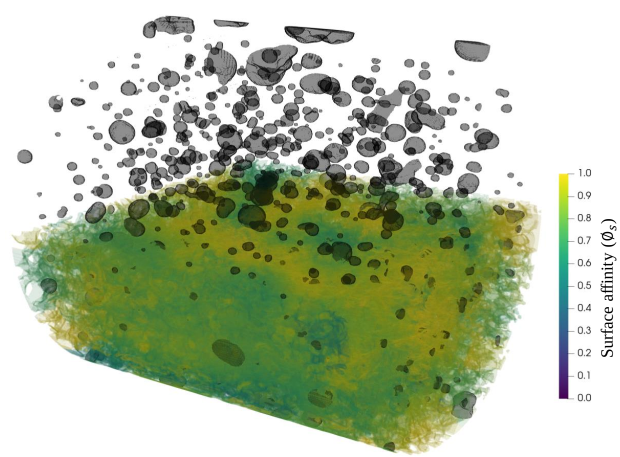

Figure 8: Surface affinity parameter (ϕ_s) distribution map for all solid-fluid voxels in the gas-water Bentheimer sample.

3.3. Oil-water Bentheimer samples (unaltered and altered)

In this section, we describe the results from running both our proposed wettability characterization workflow and from geometrical analysis on two Bentheimer samples, altered and unaltered, saturated with oil and brine. We expect the altered wettability sample to be mixed wet and the unaltered sample to be water wet [26, 53]. Figure 9 shows the obtained surface affinity distributions for altered and unaltered samples using local LB simulation on trapped ganglia. The wettability distribution of samples shows an obvious distinction between the two samples, with a shift toward oil-wetness for the altered sample, as well as a wider range showing the mixed-wet behaviour. Figure 10 depicts the obtained contact angle distributions for the altered and unaltered samples using geometrical analysis. The difference between the two samples is lower compared to Figure 9. Moreover, both distribution profiles show a wide range of obtained contact angles with a slight difference between the peak contact angle values.

Figure 11 compares all obtained contact angle distributions for altered and unaltered Bentheimer samples under oil-water fluid pair. For the unaltered sample, in which we expect a water-wet behaviour from clean Bentheimer sandstone the results of the proposed wettability characterization scheme show a stronger water-wetting behaviour compared to geometrical analysis. The same difference applies to the altered sample. The local LBM simulations show a peak contact angle distribution of around 70 degrees while the geometrical analysis distribution peaks around 90 degrees, showing a neutral wetting behaviour. In the presented results, the contact angle distribution of the unaltered sample obtained by geometrical analysis matches the obtained contact angle distribution for the altered sample using local LBM simulations. Based on the provided results we believe that the proposed scheme provides more accurate and representative results compared to geometrical analysis, which might be due to smoothing the interface along the contact line and calculation of the normal vector locally.

Finally, Figure 12 shows the obtained surface affinity parameter (ϕ_s) map for all solid-fluid voxels for half of the altered and unaltered Bentheimer samples. The solid-fluid voxels are not shown for the top half of the sample for better visualization and to be able to visualize the wetting distribution inside the sample as well as the spatial distribution of three-phase contact lines. There is a significant difference between the affinity maps with a shift toward oil-wetness for the mixed wet sample, which is expected.

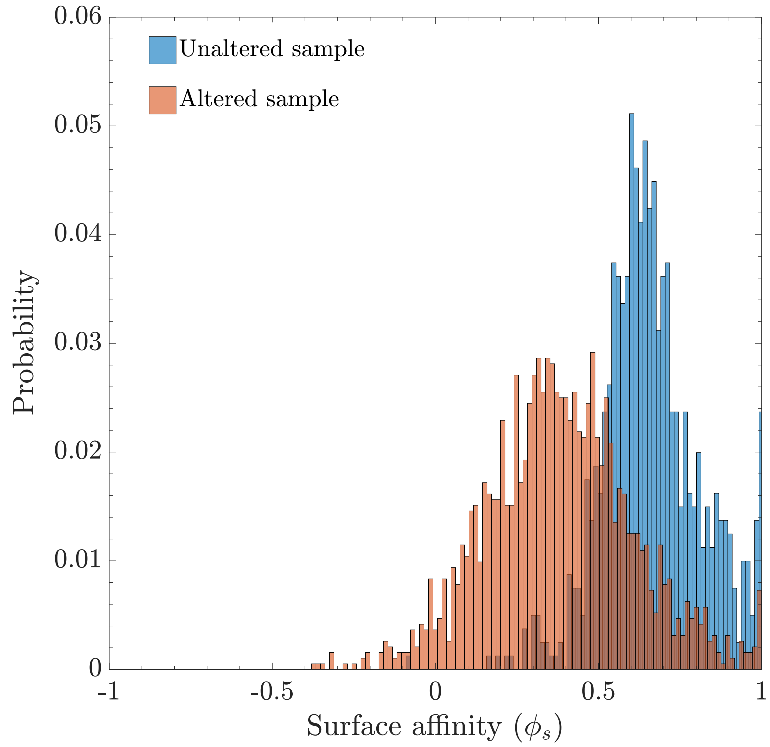

Figure 9: The distribution of obtained surface affinity parameter (ϕ_s) for altered and unaltered Bentheimer sandstone samples saturated with oil and brine phases.

4. Summary and Conclusions

This study presented a new approach to spatial characterisation of wettability in porous media. The presented workflow is computationally efficient, as it uses local lattice-Boltzmann (LB) simulations, and upscales well as it is performed on the segmented structure of rock and fluids in porous media. The developed workflow works on trapped ganglia of the non-wetting phase individually and conducts local lattice-Boltzmann simulations to obtain the most appropriate wetting parameter which describes that specific ganglion as close as possible to the observed geometry in the porous medium. We used a colour-gradient lattice-Boltzmann model to simulate two-phase fluid distribution in porous media.

To determine the local wettability in the porous medium, we isolated each disconnected ganglion of fluids and ran one LB simulation for each ganglion

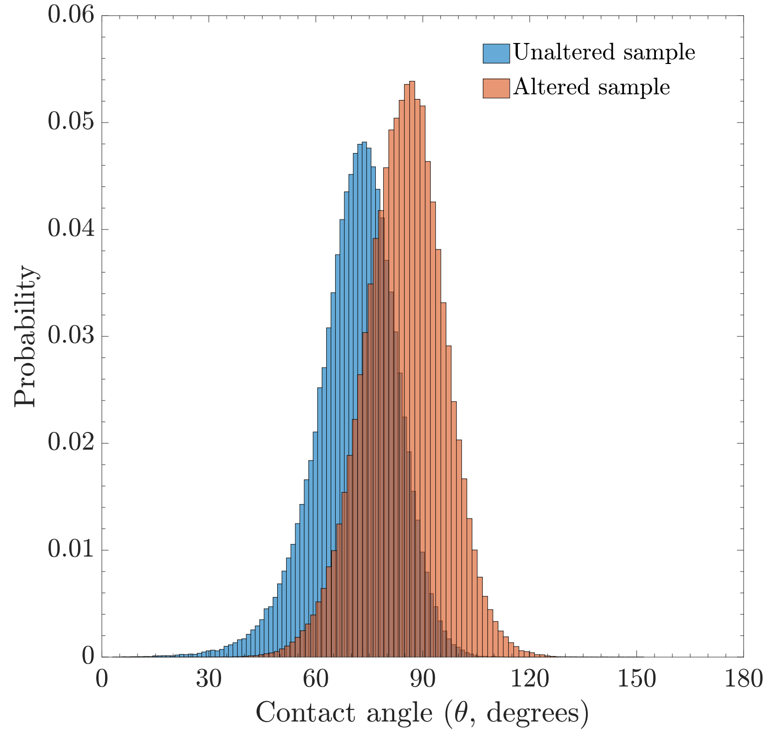

Figure 10: The contact angle distribution for altered and unaltered Bentheimer sandstone samples saturated with oil and brine phases. The contact angle distribution is obtained by geometrical contact angle determination.

in the porous medium. We optimized the surface affinity parameter (through which the wettability is imposed in the solver) for each ganglion with the aim of the best ganglion shape replicating the LB results with the imaged ganglion geometry. Using this approach, we obtained a surface affinity parameter for each disconnected ganglion and assigned it to the three-phase (fluid-fluid-solid) contact line. Computing sequentially on a single ganglion makes the method computationally advantageous and RAM-efficient, moreover it can be parallelized very efficiently to run the algorithm on multiple ganglia at the same time. After obtaining the surface affinity for all three-phase contact line voxels, the surface affinity of all solid-fluid voxels of the porous medium was estimated using 3D spatial interpolation.

First, the results of the developed workflow were compared with a geometrical contact angle (CA) determination scheme proposed by Khanamiri

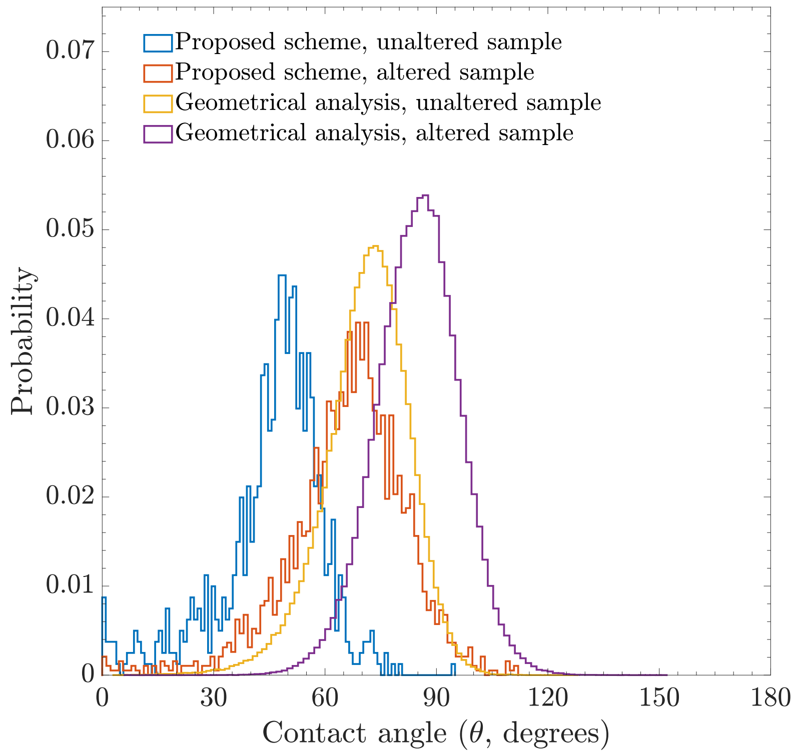

Figure 11: Contact angle distributions obtained from local LB simulations and geometrical contact angle determination schemes for altered and unaltered Bentheimer samples saturated with oil and brine phases.

et al. [32] on two synthetic cases, generated by two-phase flow simulation in a porous medium. Our analysis revealed that the results obtained from the developed workflow accurately represent both strongly wetting and intermediate wetting states, whereas the geometrical analysis struggles to capture the extreme wetting case and yields a broader spectrum of contact angles, leading to increased uncertainty. Then, three sets of experimental data were used to quantitatively compare the results of the proposed scheme with geometrical analysis. The first set of experimental data was from a Bentheimer sandstone saturated with air and water in ambient conditions. Both the proposed scheme and the geometrical analysis showed water wetness, with the former showing more water-wetting behaviour and a narrower span of contact angle distribution. It is known that natural surfaces show a strong liquid wetting behaviour in the presence of gas [55], from which we conclude that

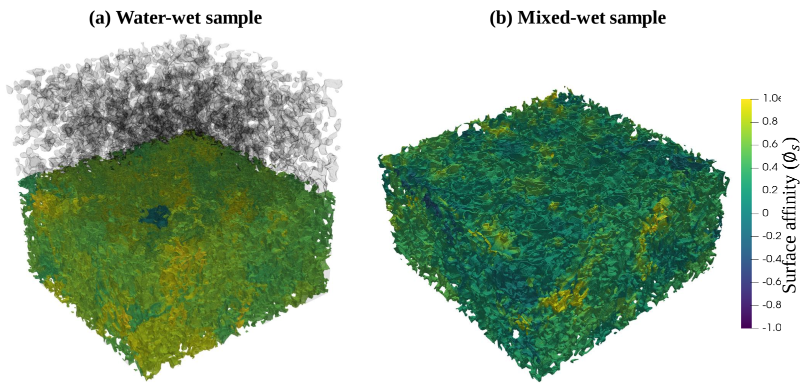

Figure 12: Surface affinity parameter (ϕ_s) distribution map for all solid-fluid voxels in the (a) unaltered and (b) altered Bentheimer samples.

the local LBM simulations provide a more realistic wettability description for this sample.

The second and third sets of experimental data were oil-water saturated unaltered and altered (aged with crude oil) Bentheimer samples under steady-state flow ($f_w = 0.5$). We expect the unaltered sample to show a water-wet behaviour while the altered sample is expected to be mixed-wet. The difference in contact angle distribution for these two samples was small when the geometrical contact angle determination was applied, while the proposed scheme showed a larger difference between the two datasets. The proposed scheme showed a water-wet behaviour for the unaltered sample while the geometrical contact angle determination showed contact angle distributions peaking around a neutral wetting state (75<CA<105). Based on the provided results we believe that the proposed scheme based on local LBM simulations provides more accurate and representative results compared to the traditional geometrical analysis.

Acknowledgements

This study was funded by the Research Council of Norway, project number 301412. Carl Fredrik Berg was funded by the Research Council of Norway Centers of Excellence funding scheme, project number 262644, PoreLab.

References

[1] T. Akai, M. J. Blunt, B. Bijeljic, Pore-scale numerical simulation of low salinity water flooding using the lattice Boltzmann method, Journal of Colloid and Interface Science 566 (2020) 444–453.

[2] R. Aziz, V. Niasar, H. Erfani, P. J. Martínez-Ferrer, Impact of pore morphology on two-phase flow dynamics under wettability alteration, Fuel 268 (2020) 117315.

[3] A. Golparvar, Y. Zhou, K. Wu, J. Ma, Z. Yu, A comprehensive review of pore scale modeling methodologies for multiphase flow in porous media, Advances in Geo-Energy Research 2 (2018) 418–440.

[4] M. Celia, S. Bachu, J. Nordbotten, K. Bandilla, Status of CO_2 storage in deep saline aquifers with emphasis on modeling approaches and practical simulations, Water Resources Research 51 (2015) 6846–6892.

[5] S. Krevor, M. J. Blunt, S. M. Benson, C. H. Pentland, C. Reynolds, A. Al-Menhali, B. Niu, Capillary trapping for geologic carbon dioxide storage–from pore scale physics to field scale implications, International Journal of Greenhouse Gas Control 40 (2015) 221–237.

[6] A. Sáinz-García, E. Abarca, V. Rubí, F. Grandia, Assessment of feasible strategies for seasonal underground hydrogen storage in a saline aquifer, International Journal of Hydrogen Energy 42 (2017) 16657–16666.

[7] L. Hashemi, M. Blunt, H. Hajibeygi, Pore-scale modelling and sensitivity analyses of hydrogen-brine multiphase flow in geological porous media, Scientific Reports 11 (2021) 1–13.

[8] D. Niblett, A. Mularczyk, V. Niasar, J. Eller, S. Holmes, Two-phase flow dynamics in a gas diffusion layer-gas channel-microporous layer system, Journal of Power Sources 471 (2020) 228427.

[9] P. P. Mukherjee, Q. Kang, C.-Y. Wang, Pore-scale modeling of two-phase transport in polymer electrolyte fuel cells—progress and perspective, Energy & Environmental Science 4 (2011) 346–369.

[10] L. Chen, Y. He, W.-Q. Tao, P. Zelenay, R. Mukundan, Q. Kang, Pore-scale study of multiphase reactive transport in fibrous electrodes of vanadium redox flow batteries, Electrochimica Acta 248 (2017) 425–439.

[11] G. Qiu, C. Dennison, K. Knehr, E. Kumbur, Y. Sun, Pore-scale analysis of effects of electrode morphology and electrolyte flow conditions on performance of vanadium redox flow batteries, Journal of Power Sources 219 (2012) 223–234.

[12] M. J. Blunt, B. Bijeljic, H. Dong, O. Gharbi, S. Iglauer, P. Mostaghimi, A. Paluszny, C. Pentland, Pore-scale imaging and modelling, Advances in Water Resources 51 (2013) 197–216.

[13] H. Andrä, N. Combaret, J. Dvorkin, E. Glatt, J. Han, M. Kabel, Y. Keehm, F. Krzikalla, M. Lee, C. Madonna, et al., Digital rock physics benchmarks—Part I: Imaging and segmentation, Computers & Geosciences 50 (2013) 25–32.

[14] A. Q. Raeini, M. J. Blunt, B. Bijeljic, Direct simulations of two-phase flow on micro-CT images of porous media and upscaling of pore-scale forces, Advances in Water Resources 74 (2014) 116–126.

[15] R. T. Armstrong, J. E. McClure, M. A. Berrill, M. Rücker, S. Schlüter, S. Berg, Beyond darcy's law: The role of phase topology and ganglion dynamics for two-fluid flow, Physical Review E 94 (2016) 043113.

[16] J. E. McClure, R. T. Armstrong, M. A. Berrill, S. Schlüter, S. Berg, W. G. Gray, C. T. Miller, Geometric state function for two-fluid flow in porous media, Physical Review Fluids 3 (2018) 084306.

[17] T. Bultreys, Q. Lin, Y. Gao, A. Q. Raeini, A. AlRatrout, B. Bijeljic, M. J. Blunt, Validation of model predictions of pore-scale fluid distributions during two-phase flow, Physical Review E 97 (2018) 053104.

[18] Z. Liu, A. Herring, C. Arns, S. Berg, R. T. Armstrong, Pore-scale characterization of two-phase flow using integral geometry, Transport in Porous Media 118 (2017) 99–117.

[19] C. F. Berg, O. Lopez, H. Berland, Industrial applications of digital rock technology, Journal of Petroleum Science and Engineering 157 (2017) 131–147.

[20] A. Cassie, S. Baxter, Wettability of porous surfaces, Transactions of the Faraday Society 40 (1944) 546–551.

[21] K. S. Sorbie, A. Skauge, Can network modeling predict two-phase flow functions?, Petrophysics-The SPWLA Journal of Formation Evaluation and Reservoir Description 53 (2012) 401–409.

[22] I. Bondino, G. Hamon, W. Kallel, D. Kac, Relative permeabilities from simulation in 3D rock models and equivalent pore networks: critical review and way forward, Petrophysics-The SPWLA Journal of Formation Evaluation and Reservoir Description 54 (2013) 538–546.

[23] R. T. Armstrong, C. Sun, P. Mostaghimi, S. Berg, M. Rücker, P. Luckham, A. Georgiadis, J. E. McClure, Multiscale characterization of wettability in porous media, Transport in Porous Media 140 (2021) 215–240.

[24] M. Andrew, B. Bijeljic, M. J. Blunt, Pore-scale contact angle measurements at reservoir conditions using X-ray microtomography, Advances in Water Resources 68 (2014) 24–31.

[25] G. Garfi, C. M. John, S. Berg, S. Krevor, The sensitivity of estimates of multiphase fluid and solid properties of porous rocks to image processing, Transport in Porous Media 131 (2020) 985–1005.

[26] G. Garfi, C. M. John, M. Rücker, Q. Lin, C. Spurin, S. Berg, S. Krevor, Determination of the spatial distribution of wetting in the pore networks of rocks, Journal of Colloid and Interface Science 613 (2022) 786–795.

[27] M. J. Blunt, Q. Lin, T. Akai, B. Bijeljic, A thermodynamically consistent characterization of wettability in porous media using high-resolution imaging, Journal of Colloid and Interface Science 552 (2019) 59–65.

[28] J. Schmatz, J. L. Urai, S. Berg, H. Ott, Nanoscale imaging of pore-scale fluid-fluid-solid contacts in sandstone, Geophysical Research Letters 42 (2015) 2189–2195.

[29] N. R. Morrow, The effects of surface roughness on contact: angle with special reference to petroleum recovery, Journal of Canadian Petroleum Technology 14 (1975).

[30] S.-Y. Yang, G. Hirasaki, S. Basu, R. Vaidya, Mechanisms for contact angle hysteresis and advancing contact angles, Journal of Petroleum Science and Engineering 24 (1999) 63–73.

[31] K. Singh, B. Bijeljic, M. J. Blunt, Imaging of oil layers, curvature and contact angle in a mixed-wet and a water-wet carbonate rock, Water Resources Research 52 (2016) 1716–1728.

[32] H. H. Khanamiri, P. A. Slotte, C. F. Berg, Contact angles in two-phase flow images, Transport in Porous Media 135 (2020) 535–553.

[33] C. Sun, J. E. McClure, P. Mostaghimi, A. L. Herring, M. Shabaninejad, S. Berg, R. T. Armstrong, Linking continuum-scale state of wetting to pore-scale contact angles in porous media, Journal of Colloid and Interface Science 561 (2020) 173–180.

[34] M. J. Blunt, T. Akai, B. Bijeljic, Evaluation of methods using topology and integral geometry to assess wettability, Journal of Colloid and Interface Science 576 (2020) 99–108.

[35] C. Sun, J. E. McClure, P. Mostaghimi, A. L. Herring, S. Berg, R. T. Armstrong, Probing effective wetting in subsurface systems, Geophysical Research Letters 47 (2020) no–no.

[36] C. Sun, J. E. McClure, P. Mostaghimi, A. L. Herring, D. E. Meisenheimer, D. Wildenschild, S. Berg, R. T. Armstrong, Characterization of wetting using topological principles, Journal of Colloid and Interface Science 578 (2020) 106–115.

[37] C. Sun, J. McClure, S. Berg, P. Mostaghimi, R. T. Armstrong, Universal description of wetting on multiscale surfaces using integral geometry, Journal of Colloid and Interface Science 608 (2022) 2330–2338.

[38] A. Mascini, V. Cnudde, T. Bultreys, Event-based contact angle measurements inside porous media using time-resolved micro-computed tomography, Journal of Colloid and Interface Science 572 (2020) 354–363.

[39] I. Zacharoudiou, E. S. Boek, Capillary filling and haines jump dynamics using free energy lattice Boltzmann simulations, Advances in water resources 92 (2016) 43–56.

[40] I. Zacharoudiou, E. S. Boek, J. Crawshaw, The impact of drainage displacement patterns and Haines jumps on CO_2 storage efficiency, Scientific reports 8 (2018) 1–13.

[41] S. Foroughi, B. Bijeljic, M. J. Blunt, Pore-by-pore modelling, validation and prediction of waterflooding in oil-wet rocks using dynamic synchrotron data, Transport in Porous Media 138 (2021) 285–308.

[42] A. K. Gunstensen, D. H. Rothman, S. Zaleski, G. Zanetti, Lattice Boltzmann model of immiscible fluids, Phys. Rev. A 43 (1991) 4320–4327.

[43] J. E. McClure, Z. Li, M. Berrill, T. Ramstad, The LBPM software package for simulating multiphase flow on digital images of porous rocks, Computational Geosciences 25 (2021) 871–895.

[44] J. Yang, E. S. Boek, A comparison study of multi-component lattice Boltzmann models for flow in porous media applications, Computers & Mathematics with Applications 65 (2013) 882–890.

[45] H. Huang, M. Sukop, X. Lu, Multiphase lattice Boltzmann methods: Theory and application (2015).

[46] T. Ramstad, C. F. Berg, K. Thompson, Pore-scale simulations of single-and two-phase flow in porous media: approaches and applications, Transport in Porous Media 130 (2019) 77–104.

[47] P. Lallemand, L.-S. Luo, Theory of the lattice Boltzmann method: Dispersion, dissipation, isotropy, Galilean invariance, and stability, Physical Review E 61 (2000) 6546.

[48] M. Latva-Kokko, D. H. Rothman, Static contact angle in lattice Boltzmann models of immiscible fluids, Physical Review E 72 (2005) 046701.

[49] C. F. Berg, P. A. Slotte, H. H. Khanamiri, Geometrically derived efficiency of slow immiscible displacement in porous media, Physical Review E 102 (2020) 033113.

[50] A. AlRatrout, A. Q. Raeini, B. Bijeljic, M. J. Blunt, Automatic measurement of contact angle in pore-space images, Advances in Water Resources 109 (2017) 158–169.

[51] M. Meyer, M. Desbrun, P. Schröder, A. H. Barr, Discrete differential-geometry operators for triangulated 2-manifolds, in: Visualization and mathematics III, Springer, 2003, pp. 35–57.

[52] Q. Lin, B. Bijeljic, R. Pini, M. J. Blunt, S. Krevor, Imaging and measurement of pore-scale interfacial curvature to determine capillary pressure simultaneously with relative permeability, Water Resources Research 54 (2018) 7046–7060.

[53] Q. Lin, B. Bijeljic, S. Berg, R. Pini, M. J. Blunt, S. Krevor, Minimal surfaces in porous media: Pore-scale imaging of multiphase flow in an altered-wettability Bentheimer sandstone, Physical Review E 99 (2019) 063105.

[54] Q. Lin, B. Bijeljic, S. C. Krevor, M. J. Blunt, M. Rücker, S. Berg, A. Coorn, H. Van Der Linde, A. Georgiadis, O. B. Wilson, A new waterflood initialization protocol with wettability alteration for pore-scale multiphase flow experiments, Petrophysics-The SPWLA Journal of Formation Evaluation and Reservoir Description 60 (2019) 264–272.

[55] H. Erfani, M. H. Ghazanfari, F. Karimi Malekabadi, Wettability alteration of reservoir rocks to gas wetting condition: A comparative study, The Canadian Journal of Chemical Engineering 96 (2018) 997–1004.

Annotated changes

Reply to reviewers